

SIMULATION OF THE JAPAN SEA CIRCULATION IN SUMMER 1999 USING THE MHI LAYERED MODEL

Ponomarev V.I.¹, Trusenkova O.O.¹, Talley L.D.²

¹ Pacific Oceanological Institute, Far Eastern Branch, Russian Academy of Sciences, Vladivostok, Russia

² Scripps Institute of Oceanography, La Jolla, USA

Introduction

The CREAMS project new findings concerning the Japan/East Sea (JES) circulation, water structure and variability are published in the special issue of *Journal of Oceanography*, 1999, vol. 55, N 2. Reports on climate change in JES and the adjacent area were earlier presented at the CREAMS Symposia and in the Proc. by many authors (Danchenkov *et al.*, 1996; Ponomarev *et al.*, 1996; Ponomarev & Salyuk, 1997; Minobe, 1996; Dyakov, 1996; Varlamov *et al.*, 1997; Kim & Kim, 1997; Riser, 1997; Zuenko, 1999; and others). Side by side with other numerous observational evidence, current oceanographic conditions in the sea are represented by observations in the spring 1999 cruise of R/V "Pavel Gordienko", summer 1999 cruises of R/V "Roger Revelle" and "Professor Khromov", and winter 2000 cruise of R/V "Professor Khromov" implemented in frame of the International Joint JES Project (Principal Investigator L. Talley). Analyses of these data can show JES contemporary climatic state in detail and provide a foundation for simulation of new circulation patterns, including those in the northwest sea.

Different kinds of numerical models have been applied to JES circulation study during two last decades (Yoon, 1982, 1991; Vasilyev & Makashin, 1992; Seung & Kim, 1993; Holloway *et al.*, 1995; Mooers & Kang, 1997; Hogan & Hurlburt, 1997; Kim & Seung, 1999; Kim & Yoon, 1999; and others). Well known large scale circulation patterns of the southern JES, such as the Tsushima Current Branches and deep countercurrents below, were pretty well simulated by many models. Sometimes oceanographic observations in the subtropical sea area were performed basing on modeling results. At the same time, in the northwest sea most models show only general cyclonic gyre. Different models even under similar external forcing simulate current features in the subarctic and transitional zones quite differently. That is due to thin pycnocline in this area and high sensitivity of real circulation and model solution to external forcing and the state of the sea itself.

The goal of this study is to simulate large scale circulation in the northwest JES associated with modern oceanographic conditions in the sea. For that purpose we apply the MHI layered numerical model under buoyancy forcing from the atmosphere and water exchange through the straits. Seasonally changing circulation and water structure is simulated starting from initial 3D density distribution based on oceanographic observations in summer 1999. Comparison is made with the longterm model run starting from horizontally homogeneous initial condition.

MHI Hydrodynamic Model

The MHI numerical circulation model is developed in the Marine Hydrophysical Institute (Sevastopol, Ukraine) by Dr. N. Shapiro belonging to the scientific school of Prof. A. Felzenbaum. The basic assumptions and principal features of this model are briefly summarized below; governing equations and numerical schemes are described in (Shapiro, 1998) and earlier papers.

This is a nonstationary model based on primitive equations under hydrostatic, Boussinesq and free surface approaches. Heat balance equation is employed for computing heat flux and water temperature at the sea surface from external atmosphere characteristics (incoming short-wave radiation, surface air temperature, wind velocity, and precipitation). At lateral open boundary associated with inlet/outlet ports, temperature and salinity of incoming water, inflow/outflow volume transport and current velocity, and layer thickness are set up in an annual cycle. In the momentum equations bi-harmonic viscosity is employed while harmonic viscosity is switched on for suppressing checkerboard noise only. Harmonic diffusion is always used in the heat and salt transfer equations.

The assumption of a layered model is that the sea consists of n layers of variable thickness, with governing equations integrated vertically within layers. The specific feature of the MHI model is that not only layer thickness but also temperature, salinity and density (buoyancy) are functions of both time and

horizontal coordinates. The layers are kept stable by employing *a priori* set “base” stratification which constrains density variations: $b_k^\sigma \leq b_k < b_{k-1}^\sigma$, where $k=2, \dots, n$ is layer number, $b_k^\sigma = \text{const}$ is k^{th} layer base buoyancy ($b_k^\sigma > b_{k+1}^\sigma$), $b_1^\sigma = \infty$, $b_n^\sigma = 0$, $b_k = b_k(x, y, t)$ is k^{th} layer buoyancy, x, y are horizontal coordinates, and t is time.

The horizontally non-uniform turbulent upper mixed layer (UML) is an important component of the MHI model. The approach to parameterization of UML dynamics and calculation of buoyancy flux at the UML lower border is, generally, similar to that developed by Bleck *et al.* (1989), with the exception of employing non-homogeneous inner layers below UML. Coupling UML with horizontally non-uniform inner layers promotes more realistic approach to subduction in the MHI model, so both entrainment and subduction modes are allowed. If layer density is out of limits specified by base buoyancy, the layer outcrops, acquiring zero thickness and becoming dynamically inactive and transparent for impulse, heat and salt fluxes, with water going to a layer of appropriate base buoyancy. Layer outcropping and layer interfaces movement upward to UML lower boundary are associated with oceanographic frontal surfaces and frontal zone formation. Winter convection is also simulated by layer outcropping under negative net heat flux at UML lower boundary and unstable stratification in upper layers. In this case, thickened UML contacts a deeper layer of corresponding density. In spring and summer sea surface heating results in positive buoyancy flux into the sea which restores outcropped layers (subduction).

Design of Numerical Experiments

Initial density distribution for the spin-up summer 1999 experiment is based on data collected in frame of the International Joint JES Project (Principal Investigator L. Talley) during the summer cruises of R/V “Roger Revelle” and “Professor Khromov”, June-August 1999. A number of layers with attributed base buoyancy are chosen to reproduce UML, subtropical water, pycnocline and deep waters in the numerical Experiments Ia and Ib with horizontal resolution of $1/4^\circ$ and $1/8^\circ$ (20-28 km and 10-14 km), respectively.

Isopycnal surfaces corresponding to the base buoyancy are taken as initial lower interfaces for inner layers, with data having been smoothed in large scale term when interpolated to the grids. Interface topography shows similar large scale features for all inner layers (see examples for the 2nd, 5th, and 7th layers in Fig. 1a-c). Those features are elevation in the Northwest JES area adjacent to the Primorye coast and depression in the southeast area associated with the Tsushima Warm Current. Initial homogeneous temperature and salinity in layers specify layer initial buoyancy (Table 1), therefore initial horizontal density gradient is set up through layer interface slopes. It should be noted that no observations were performed in the North Korea coastal area (northward 38°N and westward 131°E) or northern Tatar Strait (northward 48°N). Extrapolation to these areas is justified by smoothed large scale character of initial interface topography.

The Experiment II is set up from horizontally homogeneous initial condition for the long-term run for comparison with spin-up summer 1999 simulation. See parameters in Table 1.

Model bottom topography is introduced by scaling sea depth by the factor of α :

$$z'_d(x, y) = z_m + \alpha[z_d(x, y) - z_m],$$

where, z_m is mean sea depth;

$z_d(x, y)$ and $z'_d(x, y)$ are initial and scaled sea depth, respectively. See α in Table 1. Scaled sea depth is smoothed with 9-point linear filter (Fig. 1d).

We implemented no-wind experiments, so JES circulation is simulated as developed under buoyancy forcing through sea surface and ports only. However, non-zero wind velocity module is employed for calculating heat flux on sea surface. Note that evaporation is taken equal to precipitation in these experiments. The Tsushima (Korean) Strait is set up as an inflow port with volume transport, temperature and salinity taken varied seasonally. They are approximated for every time step by sinusoid from given extreme values for February and August (Table 1). The Tsugaru and La Perouse Straits are outflow ports dividing inflow transport by ratio of 2:1.

Parameters, initial and boundary conditions for the numerical experiments

	Experiment Ia	Experiment Ib	Experiment II
<i>Simulation parameters</i>			
Horizontal resolution	1/4°	1/8°	1/4°
Number of layers	9	7	10
Time step	15 min	1-5 min	15 min
Sea depth scaling factor α	0.3	0.5	0.3
Starting date	1 st of June		
Harmonic viscosity/diffusion coefficient	2500 m ² /s	250 m ² /s	2500 m ² /s
Bi-harmonic viscosity coefficient	2.5·10 ¹⁰ m ⁴ /s	2.5·10 ⁹ m ⁴ /s	2.5·10 ¹⁰ m ⁴ /s
Coefficient of diapycnal mixing	1-5 ·10 ⁻⁶ m/s		1-5·10 ⁻⁶ m/s
<i>Initial conditions</i>			
Layer base buoyancy	∞ , 2.4, 1.8, 1.4, 1.05, 0.87, 0.81, 0.75, 0	∞ , 2, 1.6, 1.2, 0.91, 0.79, 0	∞ ; 2.8, 2.2, 1.6, 1.2, 1.08; 0.97; 0.9; 0.85; 0
Layer initial buoyancy	4, 2.74, 2, 1.59, 1.2, 0.92, 0.84, 0.79, 0.73	3.6, 2.35, 1.8, 1.4, 1.06, 0.82, 0.77	4.3, 3, 2.8, 1.9, 1.4, 1.16, 1, 0.95, 0.89, 0.8
Initial temperature, °C	20, 15.5, 11.5, 8.5, 5.5, 2.5, 1.69, 1.07, 0.24	18.5, 13.8, 10.1, 7.1, 4, 1.4, 0.8	20, 15, 13, 9, 6, 4.5, 3, 2.5, 2, 1
Initial salinity in layers, psu	33.8, 34.22, 34.19, 34.11, 34.1, 34.06, 34.07, 34.07, 34.07	34, 34.21, 34.15, 34.1, 34.07, 34.07, 34.07	33.5, 33.65, 33.75, 33.9, 34, 34.01, 34.02, 34.035, 34.05, 34.06
Interfaces between layers, m	10 m for UML; based on 1999 summer smoothed data for inner layers (Fig. 1a-c)		10, 25, 50, 75, 100, 125, 150, 200, 250
<i>Boundary conditions on sea surface</i>			
Atmospheric fields	Climatic monthly mean incoming short-wave radiation, surface air temperature, fixed wind velocity of 5 m/s		
Wind forcing	No wind forcing experiment (wind stress is equal to zero)		
<i>Boundary conditions in ports (extreme values for February/August)</i>			
Tsushima Strait; layers 1-2	Total volume transport of 1.2/1.8 Sv; UML temperature, salinity, layer thickness of 17/22 °C, 34.6/33 psu, 74/7 m; 2 nd layer temperature, salinity, layer thickness of 17/17 °C, 34.6/34.6 psu, 1/68 m		
Tsugaru Strait; layers 1-3	UML, 2 nd and 3 rd layer thickness of 74/10 m, 1/40 m, and 25/50 m		
La Perouse Strait; layers 1-2	UML and 2 nd layer thickness of 49/7 m and 1/43 m		

Results of Numerical Experiments

The MHI model pretty well reproduces the principal currents of JES both in the 1-2 year spin-up Experiment I, starting from initial density distribution in summer 1999, and in a 40 year run from horizontally homogeneous initial condition (Experiment II), under buoyancy forcing only (no-wind experiments; Figs. 2-4). In the southern sea area, the Tsushima Current and East Korea Warm Current (EKWC) are simulated. The Tsushima Current flows along the Japanese coast in the upper layer both in summer and in winter, accompanied by a chain of alternating cyclonic and anticyclonic eddies (Figs. 2a, 3a, 4a, 4b) with underlying deep countercurrent in pycnocline (Figs. 2b, 3b). Observations of eddies in the southeast JES were reported, for example in (Isoda, 1994). It should be noted, however, that due to coarse grids and considerable sea depth smoothing (Fig. 1d), the Tsushima Branches obtained in these experiments are baroclinic branches. We yet need to increase horizontal resolution and use more realistic bottom topography in order to simulate the barotropic Nearshore Tsushima Branch over the Japanese shelf and the countercurrent below the second, Offshore Tsushima Branch as documented in (Yoon, 1991; Hase *et al.*, 1999; Kim & Yoon, 1999).

EKWC reveals 2 or 3 branches in UML and pycnocline even in Experiment Ia and II with 1/4 ° spatial resolution (Figs. 2, 3). From the traditional JES circulation schemes (Yarichin, 1980) it is known that EKWC flowing as a westward boundary current along the continental slope of the Korea Peninsula

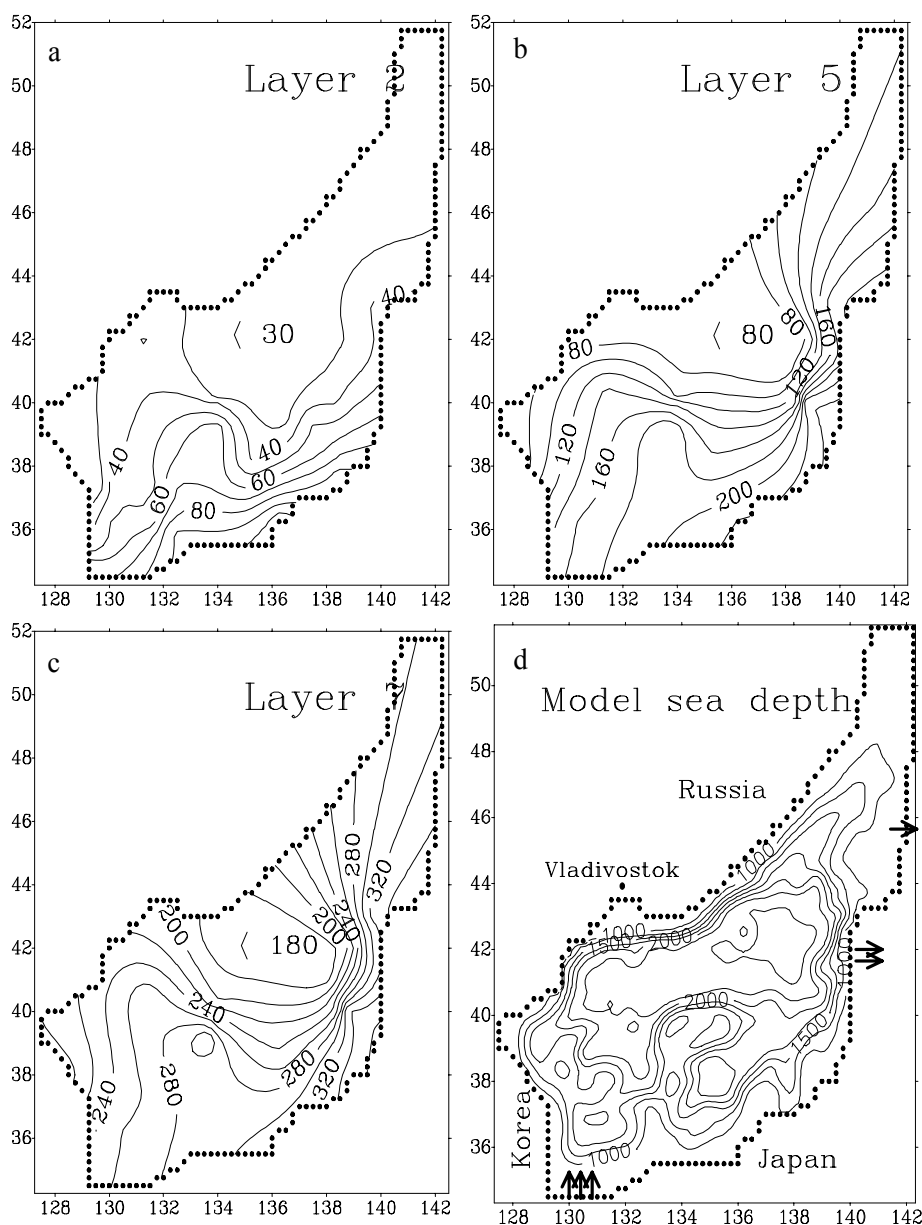


Fig. 1. Initial lower interface topography for the 2nd (a), 5th (b), and 7th (c) layers based on data from the International Joint JES Project summer cruise by R/V “Roger Revelle” and “Prof. Khromov”, June – August 1999 and the JES model bottom topography (d)

turns offshore at about 37°N. In the Experiments I-II EKWC separates from the coast at 37°30'N in summer and at 37°N in winter (Figs. 2a, 3a, 4a, 4b). However, EKWC anticyclonic meander and branches are found which carry subtropical water along the western sea coast northward as far as 40–41°N (Figs. 2a, 4a). They are revealed in UML and, even better, in pycnocline during the summer 1999 spin-up Experiment I, but not in the Experiment II long-term run. Depression corresponding to the anticyclonic meander is clearly seen in layer interfaces from UML down to the 3rd layer where it reaches 70 m depth compared to 10 m in an adjacent area (Experiment I; not shown). In the pycnocline, a southward countercurrent along the Korean coast below EKWC is simulated, propagating as far south as 35–36°N (Fig. 2b). This is in agreement with observations (Lie *et al.*, 1989) and other modeling results (Kim & Yoon, 1999).

One could consider northward EKWC propagation (Experiment I) as overshooting, the problem often arising in simulations of JES circulation. However, in the Experiment II on 1/4° grid, started from horizontally homogeneous initial condition, EKWC also separates from the Korean coast at 37°N but no northward EKWC branches develop (Fig. 3). In the same time, the southward North Korea Cold Current

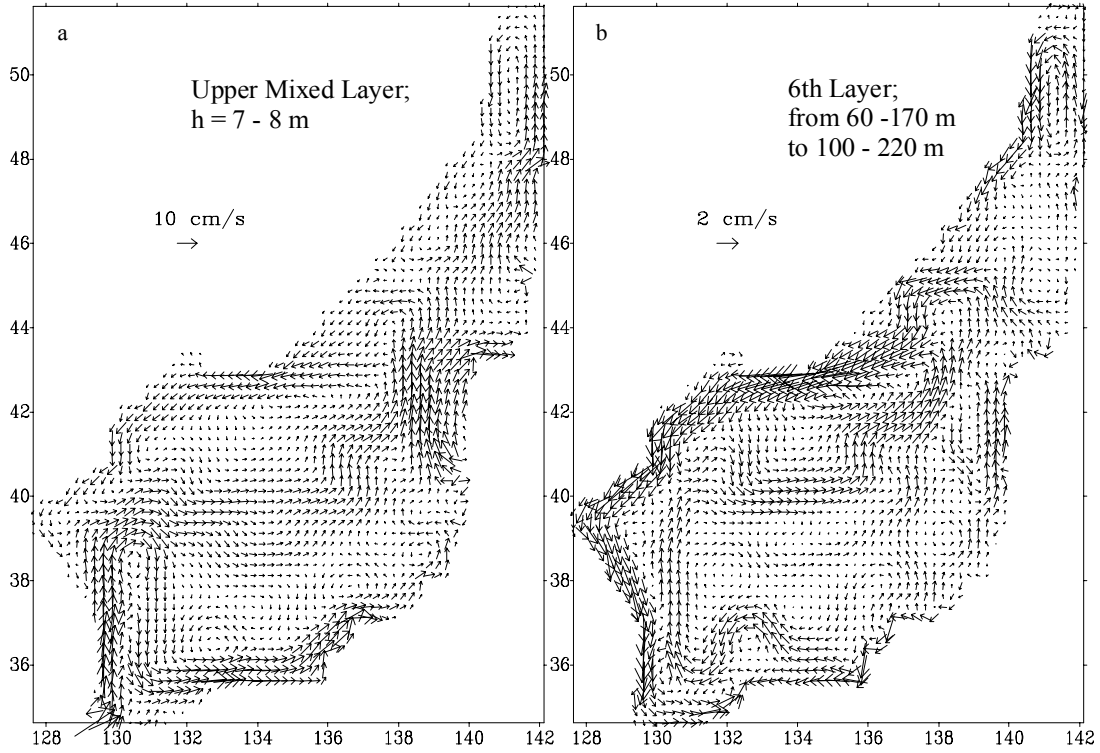


Fig. 2. Experiment Ia, $1/4^\circ$ grid. Horizontal velocity (cm/s) in the upper layer (a) and in the 6th layer (b) on August 1 after 14 months of integration

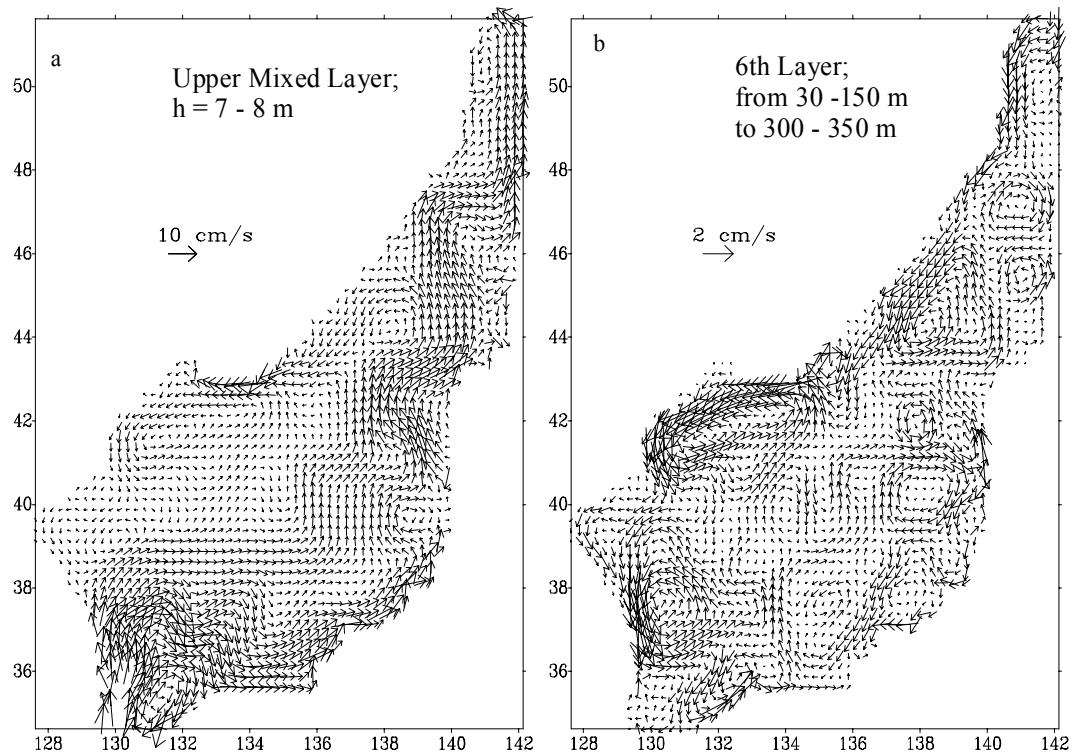


Fig. 3. Experiment II, $1/4^\circ$ grid. Horizontal velocity (cm/s) in the upper layer (a) and in the 6th layer (b) in summer after 34 years of integration

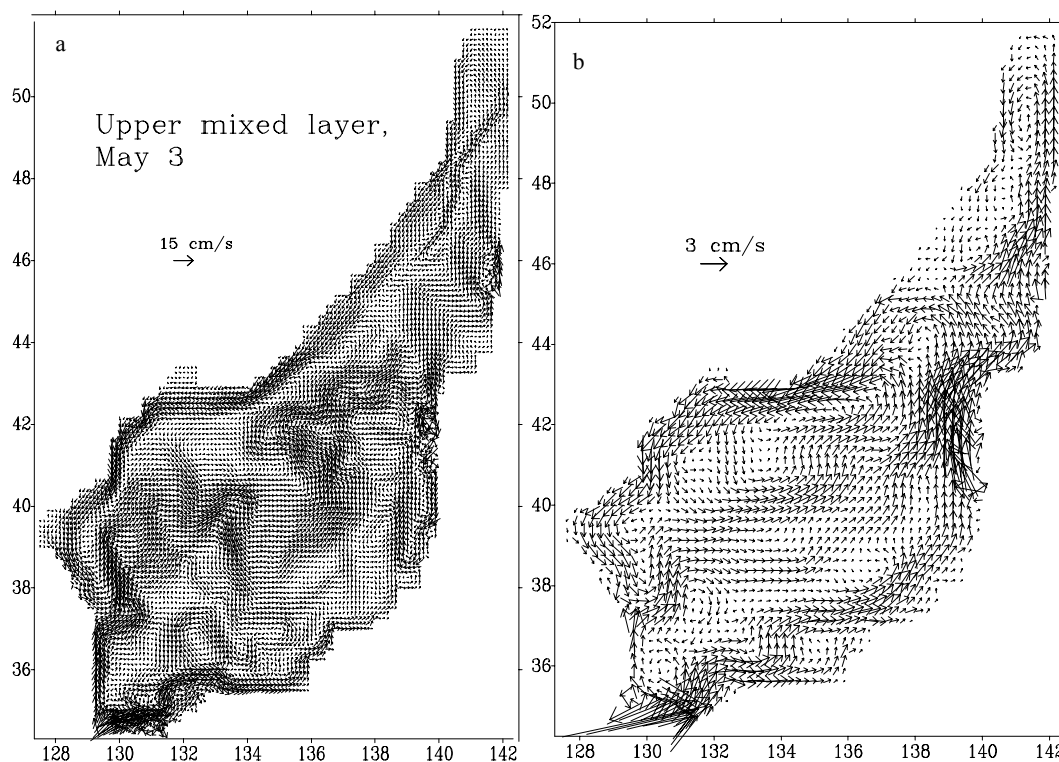


Fig. 4. Experiment Ib, $1/8^\circ$ grid (a) and Experiment Ia, $1/4^\circ$ grid (b). Horizontal velocity (cm/s) in the upper mixed layer on May 3 after 11 months of integration (a) and on February 14 after 1.5 years of integration (b)

(NKCC) flows as far to the south as $37^\circ30'N$ in the upper layer between the EKWC northward branch and the coast (Figs. 2a, 3a, 4a, 4b). In the Experiment Ib, a southeastern jet is simulated off the south Primorye coast, formed by convergence of NKCC and EKWC branches (Fig. 4a). Thermal northwest – southeast fronts were found in observations in this area, as reported by R/V “Vityaz” cruises as early as in 1950th and by Danchenkov *et al.* (2000). This jet is also seen in pycnocline (not shown). Transport of warm surface water to Peter the Great Bay area in $90^\circ S$ is clearly seen in satellite infrared images, for example in October 1996 (Danchenkov *et al.*, 1997).

The southward Primorye (Liman) Current along the Siberia coast, NKCC and EKWC close the cyclonic gyre in the northwest JES (Figs. 2-4). The multi-core structure of the cyclonic gyre is simulated, for example as a 9-core pattern in the upper layer, including one developing in the Korea Bay (Experiment Ia; Fig. 2a). Meandering of the Subarctic Front, the southern boundary of the cyclonic gyre, is clearly seen in UML and it has a distinct double structure in the pycnocline in summer and in the upper layer in winter (Figs. 2-4) reported earlier from observations (Zuenko, 1999). Warm jets forming the right-hand edge of the Subarctic Front turn westward and bring subtropical water to the Peter the Great Bay area from the east along $42^\circ30' - 43^\circ N$ and $44^\circ30' - 45^\circ N$ (Experiment Ia, Fig. 2), $43 - 43^\circ30' N$ and $44^\circ30' - 45^\circ30' N$ (Experiment II, Fig. 3), or $41 - 42^\circ N$, (Experiment Ia; Fig. 4a). As to our knowledge, no similar westward cross-cut jets were reported in previous modeling results while they were found in observations data analyses (Danchenkov *et al.*, 2000). Westward jets were also reported in the Japan Basin interior, based on satellite images (Takematsu *et al.*, 1999). Layer interface topography reflects circulation features: elevation associated with the cyclonic gyre is seen down to 8th layer, while cross-frontal sink of the 4th layer interface is from 20 to 100 m (not shown).

In the northern Tatar (Mamiya) Strait the cyclonic sub-gyre is simulated, with the southward Shrenk Current along the Siberian coast and a wider northward stream in the eastern Strait area (Figs. 2-4) which correspond to the currents found earlier in observations (Ponomarev & Yurasov, 1994). In higher resolution Experiment Ib, a narrow jet is found on this background, crossing the Tatar Strait from southwest to northeast (Fig. 4a). It carries transformed subtropical water to the northern Tatar Strait. It is known that the Tsushima Current water is of decreased oxygen while the Shrenk Current water is characterized by increased oxygen. Alternating areas of increased and decreased subsurface oxygen

consistent with these jets can be seen in the oxygen section across the Tatar Strait made in March 2000 in the R/V “Professor Khromov” cruise (Ponomarev *et al.*, 2000).

In winter the circulation system, especially the northwestern cyclonic gyre, naturally shifts southward; northward transport of subtropical water becomes less pronounced (Fig. 4b). Seasonal changes in the upper layer are clearly seen in temperature (Fig. 5a), salinity (not shown) and UML lower interface (Fig. 5b) in late February in the spin-up Experiment I as well as in long-term run Experiment II (not shown). The deepest winter convection develops in the northwest JES adjacent to the Siberian coast, the lowest SST is inside the cyclonic gyre off the Peter the Great area which implies the highest heat flux from the sea to atmosphere.

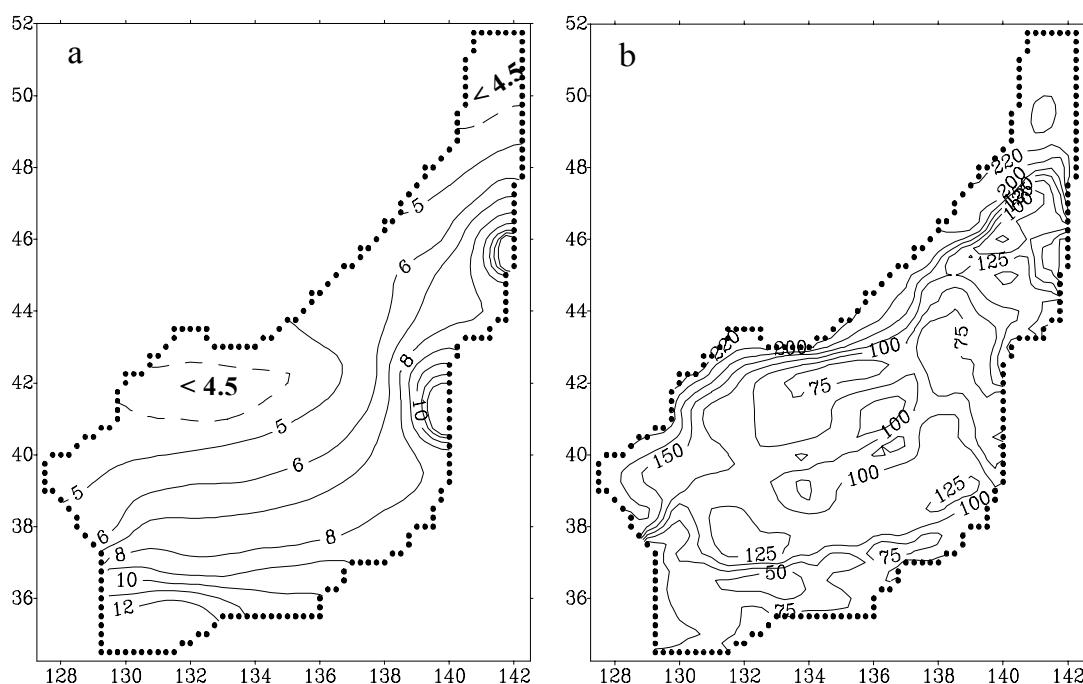


Fig. 5. Experiment Ia, $1/4^\circ$ grid. Temperature (a) and lower interface depth (b) for the upper layer on February 14 after 1.5 years of integration

Conclusion

- The general JES circulation is simulated, starting from initial condition based on data of the summer 1999 cruises (Experiment I) or from horizontally homogeneous initial condition (Experiment II), with all known currents obtained in no wind numerical experiments on $1/4^\circ$ and $1/8^\circ$ grids. Some faults of the simulations are due to coarse grids and absence of continuous shelf along the Japanese coast.
- EKWC separates from the continental coast at $37^\circ30'N$ in summer and at $37^\circ N$ in winter. However, in the spin-up Experiment I EKWC branches are simulated carrying subtropical water along the western coast northward as far as $40\text{--}41^\circ N$. No such branches are simulated in the longterm Experiment II, so they can be considered as a specific feature of circulation in 1999.
- The multi-core cyclonic gyre is simulated in the north and northwest JES, with meandering and branching of its southern boundary, the Polar (Subarctic) and Northern Fronts.
- Westward cross-cut jets are simulated in the northwest JES in the $41\text{--}44^\circ N$ latitude belt in both Experiments I and II, so this feature should not be exclusively associated with oceanographic conditions of summer 1999 but can be considered as JES persistent circulation pattern. These jets are branches of the Tsushima Current turning westward off the Tsugaru Strait adjacent area and carrying transformed subtropical water to the southern Primorye adjacent area from the east.
- Simulated winter convection reaches its maximal depth along the northwest edge of the cyclonic gyre adjacent to the Siberian coast, in particular in the area off the Peter the Great Bay.

References

1. Bleck R., Hanson H.P., Hu D. & Kraus E.B. 1989. Mixed layer-thermocline interaction in a three-dimensional isopycnic coordinate model // *J. Physical Oceanography*. Vol. 19. N 10. P. 1417-1439.
2. Danchenkov M.A., Aubrey D.G. & Lobanov V.B. 2000. Winter spatial sea-water structure of the northwest Sea of Japan // *Hydrometeorological and ecological conditions in the Far Eastern Seas: marine environmental impact assessment*. FERHRI Special Issue. N 3. Vladivostok: Dalnauka. P. 92-105.
3. Danchenkov M.A., Kim K. & Goncharenko I.A. 1996. Extremal winters in the East (Japan) Sea by monthly air temperature // *Proc. fourth CREAMS Workshop*. Vladivostok. 1996. P. 7-16.
4. Danchenkov M.A., Lobanov V.B. & Nikitin A.A. 1997. Mesoscale eddies in the Japan Sea, their role in circulation and heat transport // *Proc. CREAMS'97*. Fukuoka. Japan. P. 81-84.
5. Dyakov B.S. 1996. Year-to-year water variability of temperature and salinity the southeastern part of the Japan Sea in winters 1965-1992 // *Proc. fourth CREAMS Workshop*. Vladivostok. 1996. P. 95-99.
6. Hase H., Yoon J.H. & Kotera Y. 1999. The current structure of the Tsushima Warm Current along the Japanese coast // *J. Oceanography*. Vol. 55. N 2. P. 217-235.
7. Hogan P.J. & Hurlburt H.E. 1997. Sea of Japan circulation dynamics via the NRL layered ocean model // *Proc. CREAMS'97*. Fukuoka Japan. 1997. P. 109-112.
8. Holloway G., Sou T. & Eby M. 1995. Dynamics of circulation of the Japan Sea // *J. Marine Research*. Vol. 53. P. 539-569.
9. Isoda Y. 1994. Warm eddy movements in the Eastern Japan Sea // *J. Oceanography*. Vol. 50. P. 1-16.
10. Kim C.-H. & Seung Y.H. 1999. Formation and Movement of the ESIW as modeled by MICOM // *J. Oceanography*. Vol. 55. P. 369-382.
11. Kim C.-H. & Yoon J.H. 1999. A Numerical Modeling of the upper and the intermediate layer circulation in the East Sea // *J. Oceanography*. Vol. 55. N 2. P. 327-345.
12. Kim K.-R. & Kim K. 1997. What is happening in the East Sea (Japan Sea)?: Recent Chemical observations during CREAMS 93-96 // *J. Korean Soc. Oceanogr.* Vol. 31. P. 163-170.
13. Lie H.-J., Su M.S. & Kim C.H. 1989. Observations of southeastward deep currents off the east coast of Korea // *J. Korean Soc. Oceanogr.* Vol. 30. P. 170-183.
14. Minobe S. 1996. Interdecadal temperature variation of deep water in the Japan Sea (East Sea) // *Proc. fourth CREAMS Workshop*. Vladivostok. P. 81-88.
15. Mooers C.N.K. & Kang H.S. 1997. On the 26-sigma level POM model for Japan (East) Sea circulation // *Proc. CREAMS'97*. Fukuoka. Japan. P. 15-17.
16. Ponomarev V., Talley L., Tishchenko P., Sagalaev S., Salyuk A., Lobanov V.B. & Kaplunenko D.D. 2000. Anomalies of the Japan Sea deep water characteristics // *Abstracts of CREAMS'2000*. Vladivostok. Russia. P. 15.
17. Ponomarev V.I. & Salyuk A.N. 1997. Climate regime shifts and heat accumulation in the Sea of Japan // *Proc. CREAMS'97*. Fukuoka. Japan. P. 157-161.
18. Ponomarev V.I. & Yurasov G.I. 1994. The Tartar (Mamiya) Strait Currents // *J. Korean Society of Coastal and Ocean Engineers*. Vol. 6. N 4. P. 335-339.
19. Ponomarev V.I., Salyuk A.N. & Bychkov A.S. 1996. The Japan Sea water variability and ventilation processes // *Proc. fourth CREAMS Workshop*. Vladivostok. P. 63-69.
20. Riser S.C. 1997. Long-term variations in the deep ventilation of the Japan / East Sea // *Proc. CREAMS'97*. Fukuoka. Japan. P. 31-34.
21. Seung, Y.H. & Kim K. 1993. A numerical modeling of the East Sea circulation // *J. Oceanological Society of Korea*. Vol. 28. N 4. P. 292-304.
22. Shapiro N.B. 1998. Formation of the Black Sea general circulation considering stochastic wind stress // *Morskoy Gidrofizicheskiy J.* N 4. Sevastopol. Ukraine. P. 12-24.
23. Takematsu M., Ostrovskii A.G. & Nagano Z. 1999. Observations of eddies in the Japan Basin interior // *J. Oceanography*. Vol. 55. N 2. P. 237-246.
24. Varlamov S.M., Dashko N.A. & Kim Y.S. 1997. Climate change in the Far East and Japan Sea area for the last 50 years // *Proc. CREAMS'97*. Fukuoka. Japan. P. 163-166.
25. Vasilyev A.S. & Makashin V.P. 1992. Ventilation of the Japan Sea waters in winter // *La Mer*. Vol. 30. P. 169-177.
26. Yarichin V.G. 1980. Study of the state of the Japan Sea circulation // *Problems of Oceanography*. Ed. Pokudov V. Leningrad: Hydrometeoizdat. P. 46-61.
27. Yoon J.-H. 1991. The branching of the Tsushima Current // *Rep. RIAM of Kyushu Univ.* Vol. 38. P. 1-21.
28. Yoon, J.-H. 1982. Numerical experiment on the circulation in the Japan Sea. Part III. Mechanism of near-shore branching of the Tsushima Current // *J. Oceanography Society*. Japan. Vol. 38. P. 125-130.
29. Zuenko Yu. 1999. Two decades of Polar Front large-scale meandering in the North-western Japan Sea // *Proc. CREAMS'99*. Fukuoka. P. 68-71.